tvst

https://doi.org/10.1167/tvst.8.6.34

Article

Assessment of Corneal Fluorescein Staining in Different Dry Eye Subtypes Using Digital Image Analysis

Marco Pellegrini[1], Federico Bernabei[1], Fabiana Moscardelli[1], Aldo Vagge[2], Riccardo Scotto[2], Cristina Bovone[3–5], Vincenzo Scorcia[6], and Giuseppe Giannaccare[1–6]

[1] Ophthalmology Unit, S.Orsola-Malpighi University Hospital, University of Bologna, Bologna, Italy
[2] Eye Clinic of Genoa, Policlinico San Martino, Department of Neuroscience, Rehabilitation, Ophthalmology, Genetics, Maternal and Child Health (DiNOGMI), University of Genova, Genova, Italy
[3] Department of Ophthalmology, Ospedali Privati Forlì, Forlì, Italy
[4] Istituto Internazionale per la Ricerca e Formazione in Oftalmologia (IRFO), Forlì, Italy
[5] Department of Morphology, Surgery and Experimental Surgery, University of Ferrara, Ferrara, Italy
[6] Department of Ophthalmology, University of "Magna Graecia", Catanzaro, Italy

Correspondence: Marco Pellegrini, Ophthalmology Unit, S.Orsola-Malpighi University Hospital, University of Bologna, Via Palagi 9, 40138, Bologna, Italy. e-mail: marco.pellegrini@hotmail.it

Received: 19 March 2019
Accepted: 24 October 2019
Published: 12 December 2019

Keywords: corneal staining; ocular GVHD; Sjögren syndrome; dry eyes; image analysis

Citation: Pellegrini M, Bernabei F, Moscardelli F, Vagge A, Scotto R, Bovone C, Scorcia V, Giannaccare G. Assessment of corneal fluorescein staining in different dry eye subtypes using digital image analysis. Trans Vis Sci Tech. 2019;8(6):34, https://doi.org/10.1167/tvst.8.6.34

Purpose: To describe a new objective technique of digital image analysis for the quantification and the morphological characterization of corneal staining in the setting of dry eye disease (DED), and to apply it to distinguish Sjögren syndrome (SS) from ocular graft versus-host disease (oGVHD).

Methods: Slit-lamp photographs of corneal staining obtained from 40 patients with DED (20 with SS and 20 with oGVHD; mean age 60.7 ± 12.3 years) were evaluated. Images were subjectively graded using Oxford and National Eye Institute (NEI) scales, the staining pattern was classified as micropunctate, macropunctate, coalescent, or patch. The corneal staining index (CSI) was calculated automatically using the software ImageJ 1.51s. Particles analysis was used to calculate mean area, circularity, and roundness of staining spots.

Results: CSI was significantly correlated with Oxford and NEI scales (respectively $Rs = 0.823$ and $Rs = 0.773$; both $P < 0.001$), and showed a good interobserver reliability (intraclass correlation coefficient [ICC] = 0.988 [95% confidence interval [CI]: 0.978–0.994]). The mean area of staining spots calculated with particles analysis was significantly correlated with the subjective classification of the staining pattern ($Rs = 0.550$, $P < 0.001$). The circularity and roundness of staining spots were significantly higher in oGVHD patients compared with SS (respectively, 0.51 ± 0.11 vs. 0.44 ± 0.10, $P = 0.040$; 0.61 ± 0.03 vs. 0.59 ± 0.02, $P = 0.004$). Sensitivity and specificity to distinguish oGVHD from SS were respectively 65.0% and 60% for circularity and 80.0% and 70.0% for roundness.

Conclusions: The new algorithm showed good reliability and was well correlated with the traditional subjective grading scales. Particles analysis for the objective assessment of the staining pattern may help to differentiate patients with oGVHD from those with SS.

Translational Relevance: The digital image analysis technique may be a reliable alternative to evaluate corneal staining objectively in the clinic and in clinical trials.

Introduction

Corneal fluorescein staining (CFS) is a valuable clinical tool to assess the viability of the epithelium.[1] Punctate epithelial erosions (PEE) are a common feature of various ocular surface diseases, including dry eye disease (DED).[2–4] The elementary lesions that characterize this condition are small epithelial erosions staining with fluorescein scattered over the corneal surface, which sometimes become confluent in larger areas where single lesions are no longer visible.[5] The density and the extent of the corneal staining

provide useful information to assess disease severity and to monitor the response to treatment; additionally, its morphological pattern as well as its topographical distribution over the corneal area may provide a clue to the underlying aetiology.[6]

In the past, various grading systems have been developed for the consistent quantification of CFS severity, including the van Bijsterveld scale,[7] the National Eye Institute (NEI) scale,[8] the Oxford scale,[9] and the Sjögren's International Collaborative Clinical Alliance ocular staining score.[10] Currently, Oxford and NEI scales are the most commonly used in routine clinical practice and represent also the standards in the setting of clinical trials. However, these systems are subjective and observer dependent, being susceptible to poor reproducibility, and high interobserver and intraobserver variance.[11]

To overcome these limitations, objective methods to assess CFS based on digital image analysis have been recently developed.[12–17] All these techniques provide accurate and objective results for the quantitative grading of CFS. However, to date none of these protocols for the digital image analysis have been employed for the objective evaluation of the morphology of the staining pattern. This analysis would be of great interest to distinguish certain DED subtypes, as the other available DED diagnostic techniques (e.g., Schirmer test, break-up time) have limited capacity in the differential diagnosis of different DED etiologies. Among these, Sjögren syndrome (SS) and ocular graft versus-host disease (oGVHD), previously called Sjögren-like syndrome, represent two major causes of severe DED with similar clinical picture.[18–21]

In this study, we employed a new semiautomated method based on digital image analysis for the quantification and the morphological characterization of CFS in patients with DED owing to SS and oGVHD. The aim of the study was (1) to compare this analysis with traditional subjective grading techniques in terms of both performance and reliability for the quantification of CFS; (2) to evaluate its efficacy in identifying different CFS patterns; and (3) to compare its results in patients with SS and oGVHD.

Methods

Patients

This prospective study was conducted at the Cornea Service of the S.Orsola-Malpighi University Hospital (Bologna, Italy). Patients were included if they presented with (1) DED according to the Tear Film and Ocular Surface Society (TFOS) Dry Eye Workshop (DEWS) II Criteria[2]; (2) diagnosis of either oGVHD or primary and secondary SS; (3) CFS in at least two of the five corneal zones defined by the NEI scale (NEI score $\geq$ 2). The diagnosis of chronic oGVHD was reached according to the International Consensus Criteria on Chronic Ocular GVHD Group (ICCGVHD), which assign a score ranging from 0 to 3 points to Schirmer test, CFS and ocular surface disease index (OSDI), and a score ranging from 0 to 2 points for conjunctival injection. The diagnosis of oGVHD is reached with a total score $\geq$ 6 in the presence of systemic GVHD, and $\geq$ 8 in the absence of systemic GVHD.[22] The diagnosis of SS was reached according to the American-European Consensus Group Criteria, which identifies six criteria: (I) ocular symptoms (dry eye symptoms, foreign body sensation, use of artificial tears three or more times per day); (II) oral symptoms (dry mouth, swollen salivary glands, need for liquids to swallow dry foods); (III) ocular signs (Schirmer test $<$ 5 mm/5′, positive ocular surface staining); (IV) histopathology of salivary glands positive for focal lymphocytic sialadenitis; (V) oral signs (unstimulated whole salivary flow $\leq$1.5 mL/15′, abnormal parotid sialography, abnormal salivary scintigraphy); (VI) positivity of autoantibodies Anti-SSA (Ro) or Anti-SSB (La). The diagnosis of SS is reached with any four of the six criteria, including either item IV or VI; or with any three of the four objective criteria (III, IV, V, VI).[23]

Exclusion criteria included history of contact lens wear, previous corneal surgery, history of Stevens-Johnson syndrome, mucous membrane pemphigoid, herpetic keratitis, and active ocular allergies. In all patients, the underlying systemic disease was stable with no change of systemic therapy in the 4 weeks preceding the beginning of the study. The study was performed in accordance with the principles of the Declaration of Helsinki and was approved by the local institutional review board. Written informed consent was obtained from all patients included in the study.

Photograph Acquisition

CFS was evaluated after instillation of 20 μL unpreserved 2% sodium fluorescein. Anterior segment slit-lamp photographs were acquired with the Topcon SL-D701 photography system (Topcon Medical Systems, Inc., Oakland, NJ) using the cobalt blue

light and a 7503 Boston yellow filter. Photographs were acquired immediately after blinking, without using topical anesthesia. To standardize images, each photograph was obtained using the same magnification (×16), lighthouse angle (30°), and luminous intensity. Photographs were taken in both eyes; if both eyes were eligible, one image from one eye was selected based on satisfactory illumination, focus, and resolution.

Subjective Grading of CFS

An experienced masked investigator (FB) graded the photographs with Oxford and NEI scales. The former relies on a comparative chart to define the degree of CFS, with different images defining six levels of severity.[9] The latter relies on a chart that divides the cornea into five sections and assigns a value from 0 (absent) to 3 (severe) to each section, based on the amount, size, and confluence of the PEE, for a maximum of 15 points.[8]

Subsequently, the pattern of staining was classified as micropunctate, macropunctate, coalescent, and patch, using the method proposed by Woods et al.[24,25] Briefly, the staining type was subjectively allocated on a 0 to 100 continuous scale based on the confluence of single staining spots. A value of 1 to 25 was classified as micropunctate, 26 to 50 as macropunctate, 51 to 75 as confluent, and 76 to 100 as patch. In case of multiple staining patterns in the same image, the more represented one over the corneal area was chosen for the statistical analysis. In addition, the shape of coalescent areas and patches of staining was subjectively classified as round or oval.

Image Digital Analysis

The images were analyzed using the public domain software ImageJ 1.51s (National Institutes of Health, Bethesda, MD). Briefly, the original image was opened in ImageJ (Fig. 1A), and the oval tool was used to trace the total corneal area, which was added in the region of interest (ROI) manager and measured. Areas with specular reflections were identified, traced with the polygon tool, and added to the ROI manager. The green channel image was split from the original image; next, the contrast-limited adaptive histogram equalization was applied to highlight the pixel intensity of areas corresponding to staining, and median filtering with a 3×3 window size was applied using the "despeckle" function of the software (Fig. 1B). The MaxEntropy auto threshold function was used to obtain a binarized image (Fig. 1C). The image was then converted to a red-green-blue image, and the color threshold tool was used to select the white pixels and add them to the ROI manager. After exclusion of areas with specular reflection from the total corneal area with the "XOR" operation, the corneal staining was defined as the area of white pixels within the total corneal area. The total staining area was measured with the particle analysis function including only particles with an area $\geq$ 16 pixel^2. Finally, the CSI value, defined as the ratio between the staining area and the total corneal area, was calculated (Fig. 1D). We consider the technique to be "semiautomated" as the user has to trace manually the corneal area and areas of specular reflections.

The analysis of each image was performed separately by two investigators (MP and GG) masked to patients' characteristics, in order to evaluate the interobserver reliability. The mean value for each parameter calculated was used for the statistical analysis.

Particles Analysis

The ImageJ "Analyze Particles" function was used in attempt to describe the morphological pattern of CFS and to further differentiate patients with SS from those with oGVHD. This function allows counting and measuring objects in binary images. The analysis was applied to thresholded photographs in order to calculate the area, circularity, and roundness of single staining points. The mean values of these parameters were then obtained for each image. Briefly, circularity is defined as 4π*area/perimeter^2, whereas roundness as 4*area/(π*major axis^2). A value of circularity or roundness of 1 indicates a perfect circle; as the value approaches 0, it indicates an increasingly elongated shape. We included in this analysis only particles with an area $\geq$ 16 pixel^2. This cutoff was set to exclude smaller points, which have a value of circularity close to 1 and likely represent noise.

Statistical Analysis

The SPSS statistical software (SPSS, Inc., Chicago, IL) was used for data analysis. Values were expressed as mean $\pm$ standard deviation (SD). The interobserver reliability of the CFS digital analysis technique was evaluated using intraclass correlation coefficients (ICCs). The relationship between CSI calculated with the digital analysis technique and Oxford and NEI grading scales was evaluated using the Spearman's correlation analysis. The relationship between the

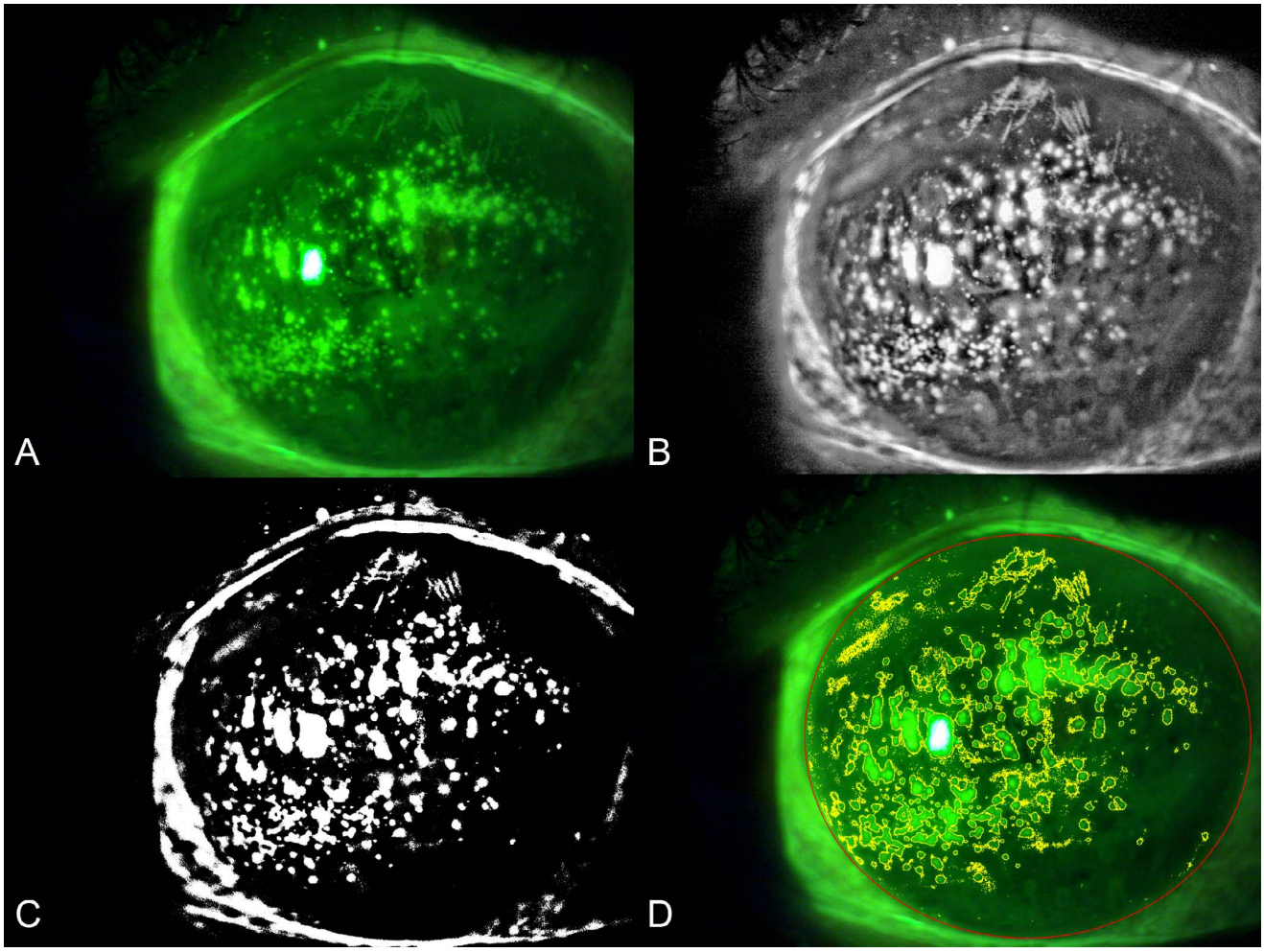

Figure 1. Representative result of the evaluation of CFS with digital image analysis. (A) Original image. (B) Contrast-limited adaptive histogram equalization and median filter were applied, and the green channel was split from the image. (C) The MaxEntropy auto threshold function was applied to binarize the image. (D) The color threshold tool was used to select the white pixels; the CSI was computed dividing the staining area (*yellow lines*) by the total corneal area (*red line*).

particles analysis results and the subjective grading of staining pattern was evaluated using the Spearman's correlation analysis. The Mann-Whitney U test was used to compare continuous and ordinal variables between patients with SS and oGVHD. The χ^2 test was used to compare dichotomous variables between patients with SS and ocular GVHD. A P value < 0.05 was considered statistically significant.

Results

A total of 40 patients with DED were included in the study (14 males and 26 females; mean age 60.7 ± 12.3 years). All patients were in treatment with tear substitutes and eyelid hygiene, 14 of them (35.0%) with topical cyclosporine, 11 (27.5%) with topical corticosteroids, 5 (12.5%) with oral omega-3 fatty acid supplementation, and 3 (7.5%) with autologous serum eye drops. Twenty patients had SS, whereas 20 patients had oGVHD. Patients with SS were significantly older than those with SS (67.4 ± 12.1 vs. 54.0 ± 8.3 years; $P = 0.001$). Sex distribution was significantly different between the two groups (19 females and 1 male in the SS group; 7 females and 13 males in the ocular GVHD group; $P < 0.001$). The mean time interval between the systemic diagnosis and the anterior segment photographs was 12.1 ± 3.2 years in patients with SS and 8.3 ± 2.5 years in patients with oGVHD.

The grade of CFS of patients with DED was 2.8 ± 1.2 according to Oxford scale, whereas 8.8 ± 2.7

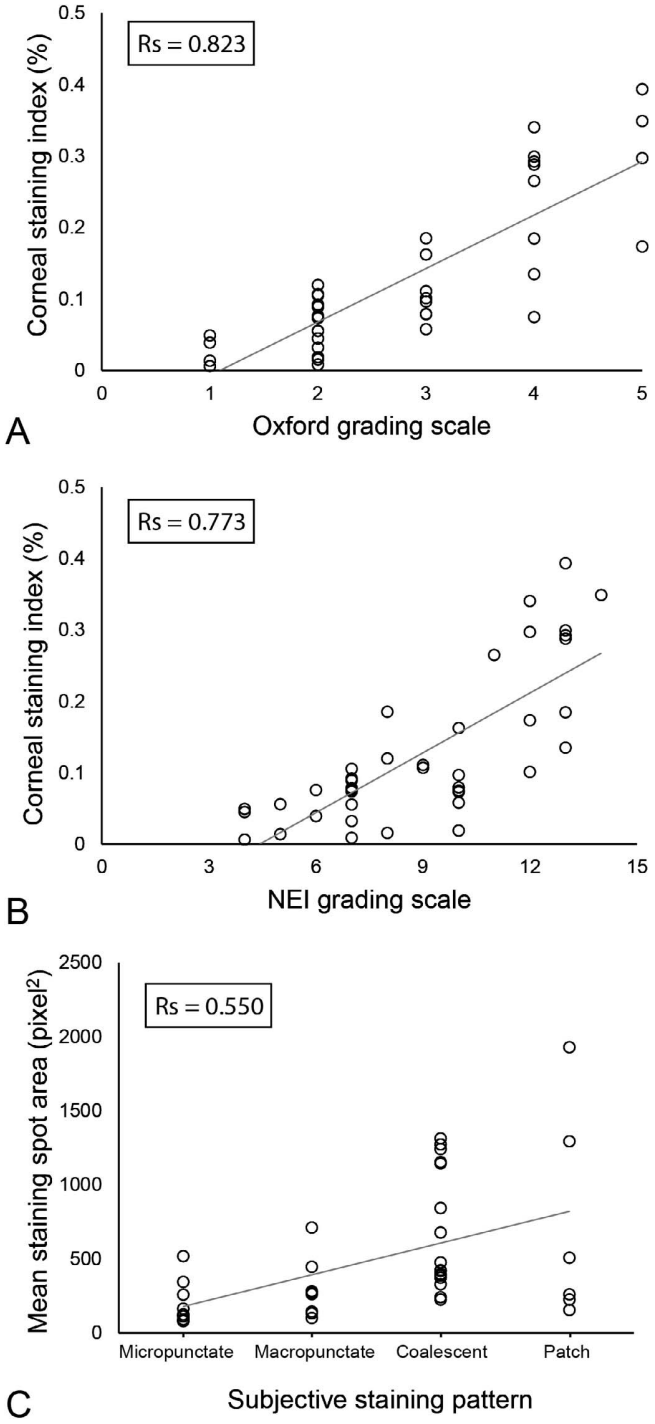

Figure 2. Scatterplots showing the relationship between the subjective grading of CFS and the results of the technique based on digital image analysis. (A) Oxford grading scale versus CSI calculated with digital image analysis ($Rs = 0.823$, $P < 0.001$). (B) NEI grading scale versus CSI calculated with digital image analysis ($Rs = 0.773$, $P < 0.001$). (C) Subjective classification of the pattern of staining versus mean area of staining spots calculated with particles analysis ($Rs = 0.550$, $P < 0.001$).

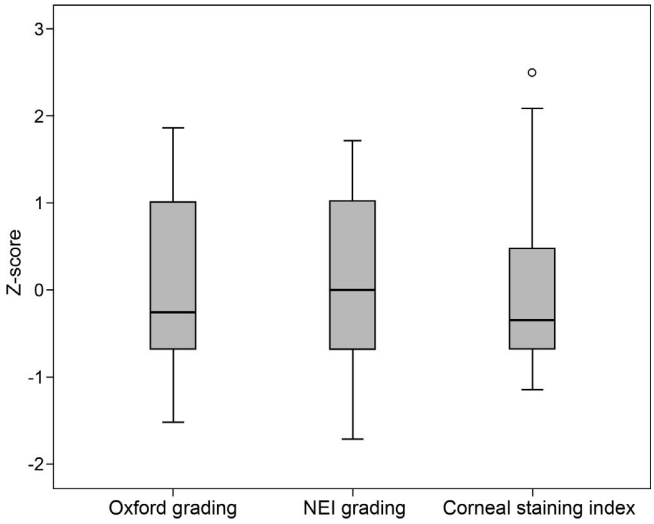

Figure 3. Boxplots showing the comparison of the Oxford scale, the NEI scale, and the CSI calculated with the digital image analysis technique to grade CFS. Variables were standardized by using the *z*-score.

according to NEI scale. The mean value of CSI calculated with the digital technique was 0.13 ± 0.11%. This parameter showed a significant correlation with both Oxford scale ($Rs = 0.823$, $P < 0.001$; Fig. 2A) and NEI scale ($Rs = 0.773$, $P < 0.001$; Fig. 2B). The digital analysis showed a good interobserver reliability when repeated by a second investigator, with an ICC of 0.988 (95% confidence interval [CI]: 0.978–0.994). Figure 3 shows the comparison of the Oxford scale, the NEI scale, and the CSI standardized by using the *z*-score.

The pattern of CFS was classified as micropunctate in 10 patients (25% of the total), macropunctate in 8 (20%), coalescent in 16 (40%), and patch in 6 (15%). The mean area, circularity, and roundness of staining spots calculated with particles analysis were respectively 489.8 ± 444.6 pixel^2, 0.47 ± 0.11, and 0.60 ± 0.03. The subjective classification of the staining pattern showed a significant correlation with the mean area of staining spots ($Rs = 0.550$, $P < 0.001$) (Fig. 2C). In particular, the mean area of staining spots was 191.4 ± 143.5 pixel^2 in eyes with a micropunctate staining pattern, and increased progressively in eyes with a macropunctate, coalescent, and patch pattern to 295.2 ± 201.7 pixel^2, 683.5 ± 407.5 pixel^2, and 730.0 ± 722.5 pixel^2, respectively. Conversely, the subjective classification of the staining pattern showed no significant correlations with circularity and roundness of staining spots (both $P > 0.05$).

Table 1. Results of the Subjective Grading of Corneal Staining in Patients With SS and oGVHD

Parameter	SS ($n = 20$)	oGVHD ($n = 20$)	P
Oxford scale, mean ± SD	2.7 ± 1.1	2.9 ± 1.3	0.718
NEI scale, mean ± SD	8.6 ± 2.9	9.1 ± 2.7	0.678
Staining pattern, no. (%)			0.312
Micropunctate	4 (20.0)	6 (30.0)	
Macropunctate	3 (15.0)	5 (25.0)	
Coalescent	8 (40.0)	8 (40.0)	
Patch	5 (25.0)	1 (5.0)	
Shape, no. (%)			0.003
Round	5 (38.5)	9 (100)	
Oval	8 (61.5)	0 (0)	

The results of the subjective grading of CFS calculated separately in the two groups of patients with SS and oGVHD are reported in Table 1. No significant differences were found between the two groups for Oxford scale, NEI scale, and the distribution of staining patterns (all $P > 0.05$). On the contrary, the shape of coalescent areas/patches of staining was subjectively classified as round in 100% of the patients with oGVHD (Fig. 4A), whereas as oval in 61.5% of patients with SS (Fig. 4B) ($P = 0.003$). All the oval areas of staining in patients with SS had a vertically oriented major axis.

The CSI and the mean area of staining spots calculated with the semiautomated method showed no significant differences between patients with SS and GVHD (respectively, 0.11 ± 0.10 vs. 0.14 ± 0.11%, $P = 0.414$; 426.1 ± 381.0 vs. 553.5 ± 502.2 pixel^2, $P = 0.383$). Conversely, patients with oGVHD showed significantly higher values of circularity and roundness of staining spots compared with those with SS (respectively, 0.51 ± 0.11 vs. 0.44 ± 0.10, $P = 0.040$; 0.61 ± 0.03 vs. 0.59 ± 0.02, $P = 0.004$; Fig. 5). Sensitivity and specificity to distinguish oGVHD from SS were respectively 65.0% and 60% for circularity and 80.0% and 70.0% for roundness.

Discussion

CFS is an important tool for both detection and grading of ocular surface disease in the routine clinical practice. As a matter of fact, it is included among the DED diagnostic criteria in the recently updated TFOS DEWS II guidelines.[2] Furthermore, CFS scores are often adopted as endpoints in the clinical trials conducted during the drug approval processes. Therefore, the quality and reliability not only of the method of staining, but also of the protocol for its grading are crucial in order to improve outcomes in DED clinical studies.

In this study, we employed an assessment of CFS based on digital image analysis. The technique is semiautomated because it requires the manual tracing of corneal area and areas of specular reflection. This new protocol demonstrated strong correlations with traditional subjective grading scales. Additionally, the interobserver reliability of the technique was good.

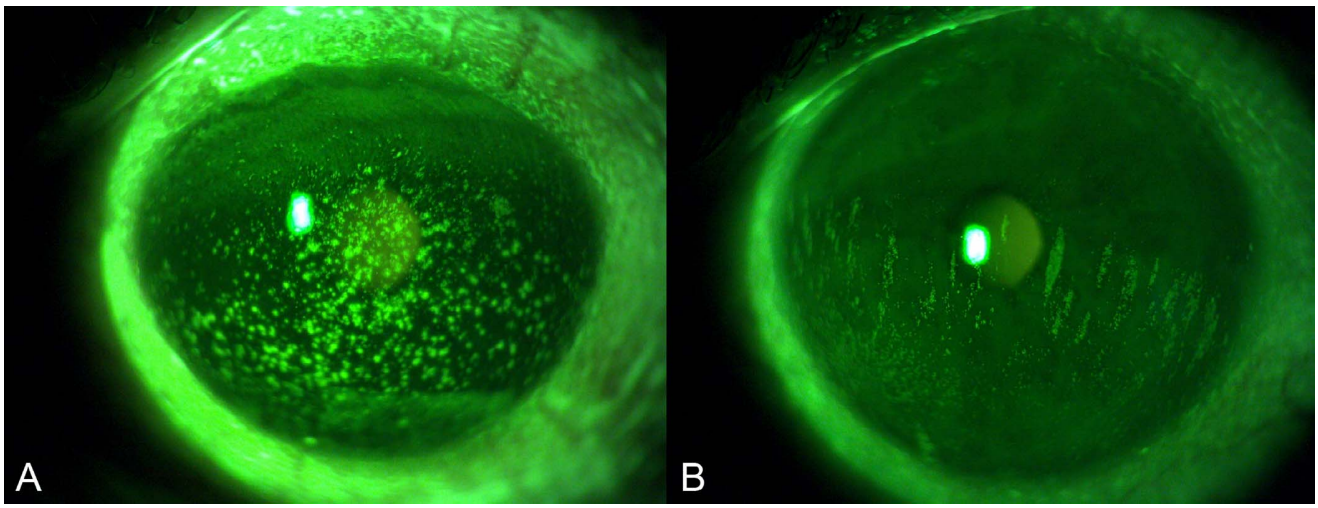

Figure 4. Representative photographs of two dry eye patients showing different patterns of staining. (A) Picture from a patient with oGVHD showed round coalescent staining spots (B). Picture from a patient with SS showed oval patches of staining with a vertically oriented major axis.

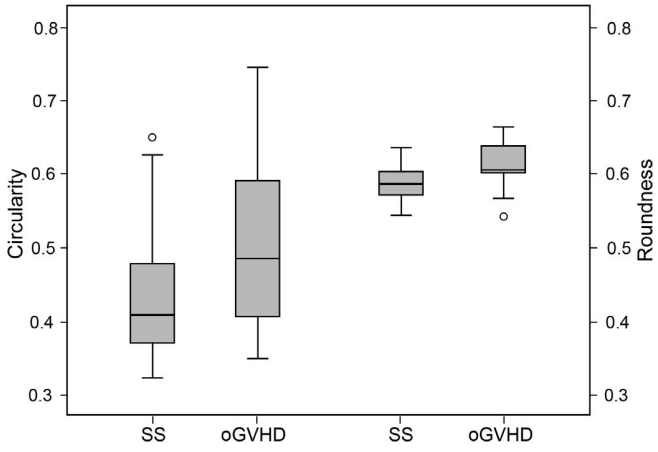

Figure 5. Boxplots showing the comparison of circularity and roundness in patients with SS and oGVHD.

Our data further confirm that the objective quantification of CFS based on digital image analysis may be suitable for its use in multicenter clinical trials, with the advantage of standardizing grading, and providing greater precision when assessing treatment efficacy.

Other previous studies reported similar results using different protocols of digital image analysis. In 2014, Chun et al.[15] developed an objective technique of CFS assessment employing the contrast-limited adaptive histogram equalization and Otsu thresholding, and showed an excellent correlation with subjecting grading scales. Rodriguez et al.[16] described a different method to detect CFS on a small area of slit-lamp photographs that also accurately reproduced a subjective grading system. Amparo et al.[17] developed another protocol combining objective CFS assessment and a continuous centesimal scale, which was more accurate in discriminating smaller differences in staining than ordinary scales with arbitrary intervals.

However, to date none of these protocols for the digital image analysis has been employed for the morphological characterization of CFS, such as coalescence and dispersion. Therefore, our technique is the first to provide an objective characterization of the staining pattern morphology. For this task, we employed the particles analysis function of ImageJ, which allows the automated measure of single staining spots in thresholded photographs. We found a significant association between the mean area of staining spots and the subjective classification of CFS pattern, with the spots' area progressively increasing from eyes with a micropunctate pattern to macropunctate, confluent, and patch pattern. However, this correlation coefficient was weaker compared with those between CSI and the Oxford scale and NEI scale. This may be due to the intrinsic limitations of the subjective classification of CFS pattern. In fact, it is very difficult to grade subjectively coalescence and dispersion in a reliable way. This further supports the utility of techniques of digital image analysis for classifying CFS pattern.

A previous study evaluated the interobserver reliability of subjective grading scales for CFS and reported good reliability of the Oxford scale and NEI scale.[26] However, all the observers in the study had approximately 10 years of clinical experience in the assessment of CFS. Conversely, digital image analysis techniques does not require any special training. In addition, it is known that subjective scales with a small number of steps typically lack sensitivity, whereas the use of scales with finer increments improves accuracy but reduces repeatability.[25]

The analysis of CFS may be helpful to provide useful information not only about the severity, but also about the etiology of certain DED subtypes. In fact, a previous study aimed at characterizing DED subtypes in relation to the localization of CFS and demonstrated that the staining of the inferior corneal area well predicted DED owing to rheumatoid arthritis, whereas its localization in the superior zone predicted thyroid disease.[27] On the contrary, other DED subtypes (i.e., SS and oGVHD) are harder to be differentiated not only using CFS alone, but also combining it with the whole armamentarium of ocular surface tests.[28] In fact, Garcia et al.[18] recently evaluated whether corneal staining combined with discomfort symptoms, Schirmer test, and break-up time could be used to distinguish DED associated with different systemic diseases. The authors concluded that those tests, even when combined, presented a limited capacity to discriminate SS and oGVHD, two overlapping DED subtypes clinically considered as "undistinguishable," in the absence of an adequate medical history collection.[18]

In our work, we used particles analysis of CFS to distinguish SS from patients with oGVHD. We found that the areas of CFS presented significantly higher circularity and roundness in patients with oGVHD compared with those with SS. This difference was detected also by the subjective evaluation of CFS pattern, according to which coalescent areas/patches of staining appeared round in the totality of eyes of patients with oGVHD, whereas appeared oval with a

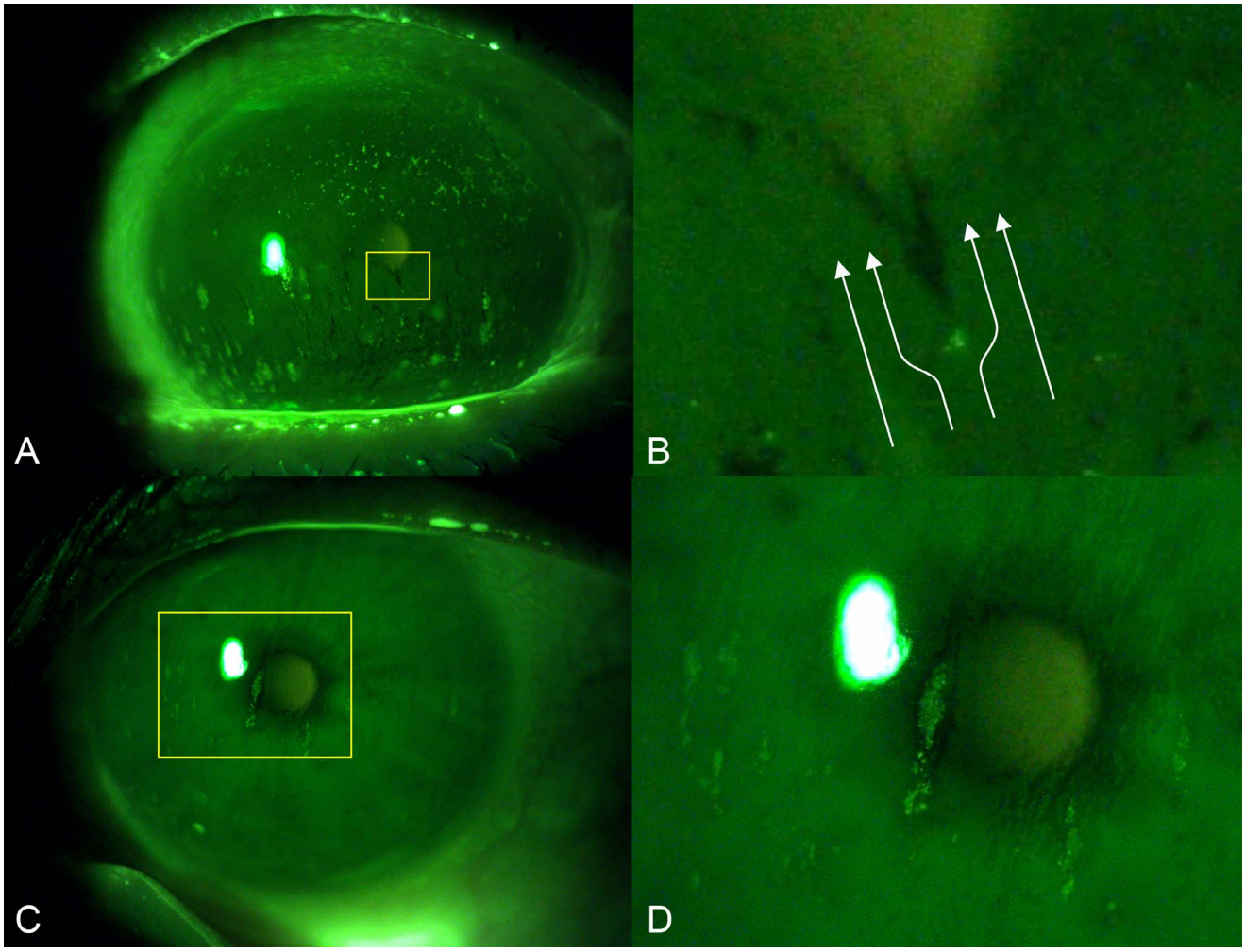

Figure 6. Hypothetical pathological mechanism leading to the formation of oval patches of staining with a vertically oriented major axis. (A) Photograph of a patient with SS taken immediately after the slower up-phase of blinking showing multiple flame shaped tear film break-up areas located above the staining spots. (B) Detail; the epithelial irregularities may act like an obstacle to the homogeneous upward movement of the tear film (represented in *white arrows*), causing the flame-shaped tear break-up in the area above the staining spot with the oval morphology. (C) Photograph of a patient with SS showing an oval patch of staining with a vertically oriented major axis. (D) Detail; the epithelial erosion may progressively enlarge over the above corneal area that remains repeatedly dry, thus creating the characteristic oval staining patch.

vertically oriented major axis in more than half eyes of patients with SS. If confirmed in larger data sets, this finding, herein described for the first time, may have useful implications in DED clinical practice. For instance, clinicians recognizing this sign in patients with DED with an undiagnosed systemic disease may consider referral for rheumatologic evaluation. However, the totality of our patients with SS had a biopsy-proven diagnosis and a long history of the disease. Therefore, this characteristic CFS pattern may not be present similarly during the earlier stages of SS, when the accurate differential diagnosis with other DED subtypes is particularly challenging.

The pathogenic mechanisms leading to this different pattern of CFS between two clinically similar DED subtypes is not clear. However, these oval areas of staining with a vertically oriented major axis seem to follow the upward spread of the tear film during the slower up-phase of blinking. In addition, the areas of tear film break-up have a similar shape and are typically located just above the micropunctate CFS spots (Fig. 6A). We hypothesize that the epithelial irregularities may act like an obstacle to the homogeneous upward movement of the tear film that cannot wet the zone just above the staining, causing the oval tear break-up in this area with the oval

morphology (Fig. 6B). As the disease progresses, the epithelial erosion can progressively enlarge over the above corneal area that remains repeatedly dry, thus creating the characteristic oval staining patch (Figs. 6C, 6D). However, although the hypothesis is intriguing, the reason for which this phenomenon occurs in patients with SS rather than in oGVHD ones is unknown. Furthermore, although the quantitative analysis of CFS did not significantly differ between SS and GVHD, we cannot exclude that a difference in the CFS severity may have influenced also the morphological pattern, and further studies are required to elucidate this point.

The technique for CFS analysis used in this study has some limitations. First, it is important to note that all the objective techniques used for the assessment of CFS are highly dependent on the repeatability of the whole process of image acquisition. Specifically, the standardization of variables such as fluorescein application, slit-lamp angle, magnification, luminous intensity, and camera settings is critical to ensure the quality of the results.[17] This may still constitute a barrier to the widespread adoption of these techniques of CFS assessment among different centers. It would have been appropriate evaluating the interobserver reliability of the whole procedure, by repeating the image acquisition in each patient and by analyzing the new images. However, only one picture per patient was acquired, and this represents a limitation of the study design. Finally, the technique that we used was not fully automated because it required the manual tracing of corneal area and the exclusion of areas of specular reflection.

In conclusion, the digital imaging analysis technique described in this study provided a reliable way of improving the clinical evaluation of CFS. The technique was well correlated with the major subjective grading scales. The new algorithm based on the particle analysis may help to differentiate patients with oGVHD and SS, two DED subtypes traditionally judged as "undistinguishable." In the future, the implementation of this technique in a wider range of ocular surface diseases might have potential applications to distinguish also other DED subtypes.

Acknowledgments

Disclosure: **M. Pellegrini**, None; **F. Bernabei**, None; **F. Moscardelli**, None; **A. Vagge**, None; **R. Scotto**, None; **C. Bovone**, None; **V. Scorcia**, None; **G. Giannaccare**, None

References

1. Pflugfelder SC. Advances in the diagnosis and management of keratoconjunctivitis sicca. *Curr Opin Ophthalmol*. 1998;9:50–53.
2. Wolffsohn JS, Arita R, Chalmers R, et al. TFOS DEWS II diagnostic methodology report. *Ocul Surf*. 2017;15:539–574.
3. Giannaccare G, Bonifazi F, Sessa M, et al. Dry eye disease is already present in hematological patients before hematopoietic stem cell transplantation. *Cornea*. 2016;35:638–643.
4. Versura P, Giannaccare G, Pellegrini M, Sebastiani S, Campos EC. Neurotrophic keratitis: current challenges and future prospects. *Eye Brain*. 2018;10:37–45.
5. Courrier E, Lépine T, Hor G, et al. Size of the lesions of superficial punctate keratitis in dry eye syndrome observed with a slit lamp. *Cornea*. 2016;35:1004–1007.
6. Bron AJ, Argueso P, Irkec M, Bright FV. Clinical staining of the ocular surface: mechanisms and interpretations. *Prog Retin Eye Res*. 2015;44:36–61.
7. Van Bijsterveld OP. Diagnostic tests in the Sicca syndrome. *Arch Ophthalmol*. 1969;82:10–14.
8. Lemp MP. Report of the National Eye Institute/Industry Workshop on Clinical Trials in Dry Eyes. *CLAO J*. 1995;21:221–232.
9. Bron AJ, Evans VE, Smith JA. Grading of corneal and conjunctival staining in the context of other dry eye tests. *Cornea*. 2003;22:640–650.
10. Whitcher JP, Shiboski CH, Shiboski SC, et al. A simplified quantitative method for assessing keratoconjunctivitis sicca from the Sjogren's Syndrome International Registry. *Am J Ophthalmol*. 2010;149:405–415.
11. Bailey IL, Bullimore MA, Raasch TW, Taylor HR. Clinical grading and the effects of scaling. *Invest Ophthalmol Vis Sci*. 1991;32:422–432.
12. Wolffsohn JS, Purslow C. Clinical monitoring of ocular physiology using digital image analysis. *Cont Lens Anterior Eye*. 2003;26:27–35.
13. Pritchard N, Young G, Coleman S, Hunt C. Subjective and objective measures of corneal staining related to multipurpose care systems. *Cont Lens Anterior Eye*. 2003;26:3–9.

14. Tan B, Zhou Y, Svitova T, Lin MC. Objective quantification of fluorescence intensity on the corneal surface using a modified slit-lamp technique. *Eye Contact Lens*. 2013;39:239–246.
15. Chun YS, Yoon WB, Kim KG, Park IK. Objective assessment of corneal staining using digital image analysis. *Invest Ophthalmol Vis Sci*. 2014;55:7896–7903.
16. Rodriguez JD, Lane KJ, Ousler GW III, Angjeli E, Smith LM, Abelson MB. Automated grading system for evaluation of corneal superficial punctate keratitis associated with dry eye. *Invest Ophthalmol Vis Sci*. 2015;56:2340–2347.
17. Amparo F, Wang H, Yin J, Marmalidou A, Dana R. Evaluating corneal fluorescein staining using a novel automated method. *Invest Ophthalmol Vis Sci*. 2017;58:168–173.
18. Garcia DM, Reis de Oliveira F, Módulo CM, et al. Is Sjögren's syndrome dry eye similar to dry eye caused by other etiologies? Discriminating different diseases by dry eye tests. *PLoS One*. 2018;13:e0208420.
19. Versura P, Giannaccare G, Vukatana G, Mulè R, Malavolta N, Campos EC. Predictive role of tear protein expression in the early diagnosis of Sjögren's syndrome. *Ann Clin Biochem*. 2018; 561–570.
20. Giannaccare G, Bonifazi F, Sebastiani S, et al. Meibomian gland dropout in hematological patients before hematopoietic stem cell transplantation. *Cornea*. 2018;37:1264–1269
21. Giannaccare G, Bonifazi F, Sessa M, et al. Ocular surface analysis in haematological patients before and after allogeneic hematopoietic stem cell transplantation: implication for daily clinical practice. *Eye (Lond)*. 2017;31:1417–1426.
22. Ogawa Y, Kim SK, Dana R, et al. International chronic ocular graft-versus-host disease (GVHD) Consensus group: proposed diagnostic criteria for chronic GVHD (Part I). *Sci Rep*. 2013;3:3419.
23. Vitali C, Bombardieri S, Jonsson R, et al. Classification criteria for Sjögren's syndrome: a revised version of the European criteria proposed by the American-European Consensus Group. *Ann Rheum Dis*. 2002;61:554–558.
24. Woods J, Woods C, Varikooty J, Jones L, Simpson T, Fonn D. A novel method of recording corneal staining that facilitates parametric analysis. *Optometry Vis Sci*. 2006;83: 65236.
25. Woods J, Varikooty J, Fonn D, Jones LW. A novel scale for describing corneal staining. *Clin Ophthalmol*. 2018;12:2369–2375.
26. Sook Chun Y, Park IL. Reliability of 4 clinical grading systems for corneal staining. *Am J Ophthalmol*. 2014;157:1097–1102.
27. Fenner BJ, Tong L. Corneal staining characteristics in limited zones compared with whole cornea documentation for the detection of dry eye subtypes. *Invest Ophthalmol Vis Sci*. 2013;54: 8013–8019.
28. Giannaccare G, Pellegrini M, Sebastiani S, Moscardelli F, Versura P, Campos EC. In vivo confocal microscopy morphometric analysis of corneal subbasal nerve plexus in dry eye disease using newly developed fully automated system. *Graefes Arch Clin Exp Ophthalmol*. 2019;257: 583–589.